Int. J. Heat Mass Transfer. Vol. 21, pp. 1355–1356

0017-9310/78/1001-1356 $02.00/0

SHORTER COMMUNICATION

PREDICTION OF MASS TRANSFER NEAR A ROTATING DISC AT HIGH SCHMIDT NUMBERS AND HIGH SWIRL RATES

B. I. SHARMA*
Owens–Corning Fiberglas, Technical Center, Granville, OH 43023, U.S.A.

(*Received* 17 *October* 1977 *and* 1 *March* 1978)

NOMENCLATURE

- C_μ, coefficient in the definition of μ_t;
- k, turbulence kinetic energy;
- l, length scale of turbulence;
- m, mass fraction of chemical species;
- p, static pressure;
- r, radial distance from axis of symmetry;
- Re, spin Reynolds number, $\omega r x/\nu$;
- Re_t, turbulence Reynolds number;
- Sc, Schmidt number;
- $\overline{Sh}$, average Sherwood number;
- U, velocity in the x-direction;
- u', fluctuating velocity in the x-direction;
- V_θ, velocity in the circumferential direction;
- W, velocity in the z-direction;
- x, coordinate measured along the surface;
- z, coordinate measured normal to the surface.

Greek symbols

- α, angle made by the x-direction with symmetry axis;
- ρ, density of fluid;
- ε, rate of dissipation of turbulence energy;
- μ, dynamic viscosity of fluid;
- μ_t, turbulent viscosity;
- μ_{eff}, effective viscosity;
- σ_t, turbulent Prandtl number/Schmidt number;
- σ_k, turbulent Prandtl number for turbulence energy;
- σ_ε, turbulent Prandtl number for rate of turbulence energy dissipation;
- σ_{eff}, effective Prandtl number/Schmidt number;
- ω, rotational speed;
- Γ_t, turbulent mass diffusivity.

1. INTRODUCTION

THE AUTHOR in his earlier publications [1, 2] had presented predictions of mass transfer near a rotating disc at Schmidt number of 2.4. Calculations of velocity profiles, torque coefficient and average Nusselt/Sherwood numbers were compared with the available experimental data. The turbulence models employed in [1, 2] were respectively the swirl flow version of mixing length hypothesis (MLH) and the energy-dissipation model of turbulence. It was noticed in [1, 2] that the mass-transfer predictions were satisfactory for spin Reynolds number below 5×10^5. Above this value, however, both Tien and Campbell [3] data and those of Kreith *et al.* [4] displayed a faster rate of increase with spin Reynolds number than the predictions. It was speculated that the relatively different behavior for the heat (agreement of predictions for the Nusselt number data was complete over the Reynolds number range explored in [1, 2]), and mass-transfer data was probably associated with different Prandtl/Schmidt number for the processes; 0.7 and 2.4, respectively. A possible reason for the underprediction of the rates of mass transfer was probably said to find its origin in effective viscosity becoming highly non-isotropic as the level of swirl progressively increases. The author has recently become aware of mass-transfer data of Ellison [5] at high swirl rates. The present note, therefore, attempts to answer the above questions, at least partially, by comparing Ellison's data to the predictions obtained using energy-dissipation model of turbulence.

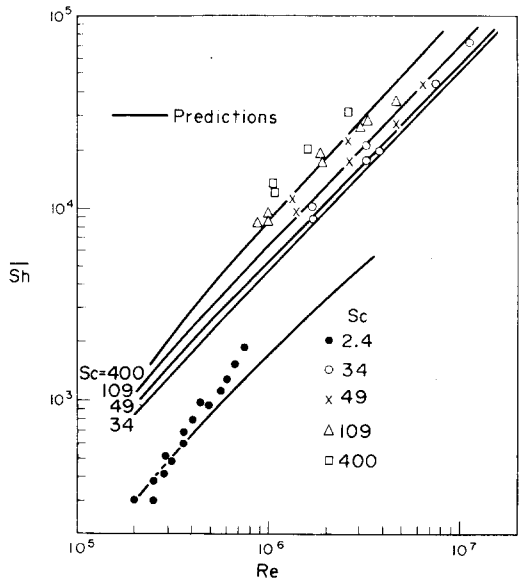

FIG. 1. Mass transfer from a rotating disc at high Schmidt numbers and high swirl rates.

2. DISCUSSION OF RESULTS

The present predictions were obtained employing energy-dissipation model of turbulence; use of mixing length hypothesis yielded virtually similar results. The finite difference numerical scheme used to solve the governing boundary layer equations is that due to Patankar and Spalding [6]. Detailed discussion of such matters appears elsewhere [1, 2]. For the convenience of the reader, however, the governing equations along with boundary conditions and the turbulence model are listed in the Appendix at the end of this note.

Figure 1 compares predictions of mass transfer with the experimental data of Ellison [5]. The data at Schmidt numbers of 34, 49, 109 and 400 were obtained at spin Reynolds number as high as 1.18×10^7. Earlier data of Tien and Campbell [3] and Kreith *et al.* [4] at Schmidt number of 2.4 are also exhibited in the figure. Ellison's data, especially for Schmidt number of 49, do exhibit some scatter. For all values of Schmidt numbers considered here, numerical predictions fall below those of experimental data. The level discrepancy being progressively larger at higher Schmidt numbers. The influence of higher swirl rates is also exhibited

*Senior scientist.

by progressively larger disagreement between data and predictions at Schmidt number of 34, 109, and 400. For Schmidt number of 2.4, it is noticed that there is close agreement between predictions and experiment for spin Reynolds number up to 4×10^5, beyond this value the data rise progressively faster than the predictions. For present calculations, the only difference between heat and mass transfer (at successively higher Schmidt numbers) processes is that the near wall region offers proportionately a much greater resistance to mass transfer than heat transfer. Earlier predictions of heat transfer [1, 2] and the present results then suggest that it is in the immediate near wall region where the turbulent transport coefficient is especially anisotropic and the turbulence models based on the effective viscosity concept break down. Therefore, to develop a model of turbulence for predicting swirling flows near solid boundaries which possess significantly greater universality than the present model, one will require the aleandonment of the isotropic effective viscosity concept. For the present case, measured profiles of species concentration near the spinning disc can more conclusively resolve this question. Since the level of disagreement between predictions and experiment here is not large (at least for moderate level of swirl rates and Schmidt numbers), it is perhaps not yet worthwhile to test complex and expensive turbulence models based on the solution of transport equations for each of the non-zero Reynolds stress components, including turbulent exchange flux $(-\overline{u'm'})$ of m.

REFERENCES

1. M. L. Koosinlin, B. E. Launder and B. I. Sharma, Prediction of momentum, heat and mass transfer in swirling turbulent boundary layers, *J. Heat Transfer* **96**, 204–209 (1974).
2. B. E. Launder and B. I. Sharma, Application of the energy dissipation model of turbulence to the calculation of flow near a spinning disc, *Letters Heat Mass Transfer* **1**, 131–138 (1974).
3. C. L. Tien and D. T. Campbell, Heat and mass transfer from rotating cones, *J. Fluid Mech.* **17**, 105 (1963).
4. F. Kreith, J. H. Taylor and J. P. Chong, Heat and mass transfer from a rotating disc, *J. Heat Transfer* **81** (1959).
5. B. Ellison, Mass transfer to a rotating disc, Ph.D. dissertation, University of California, Berkeley (1969).
6. S. V. Patankar and D. B. Spalding, *Heat and Mass Transfer in Boundary Layers*, Intertext, London (1970).
7. B. E. Launder, C. H. Priddin and B. I. Sharma, The calculation of turbulent boundary layers on spinning and curved surfaces, *J. Fluid Engng*, 231–239 (1977).
8. B. I. Sharma, Unpublished work, Mechanical Department. Imperial College of Science and Technology, London (1973).

APPENDIX

The following is the system of mean flow conservation equations (A1–A3) solved simultaneously with equations (A4–A7), describing the turbulence quantities constituting the energy-dissipation model of turbulence. Complete details can be found in [1, 2].

Streamwise momentum:

$$\rho U\frac{\partial U}{\partial x}+\rho W\frac{\partial U}{\partial z} = -\frac{\partial p}{\partial x}+\frac{1}{r}\frac{\partial}{\partial z}\left[r\mu_{\text{eff}}\frac{\partial U}{\partial z}\right]+\frac{\rho V_\theta^2}{r}\sin\alpha. \quad \text{(A1)}$$

Angular momentum:

$$\rho U\frac{\partial (rV_\theta)}{\partial x}+\rho W\frac{\partial (rV_\theta)}{\partial z}=\frac{1}{r}\frac{\partial}{\partial z}\left[r^3\mu_{\text{eff}}\frac{\partial (V_\theta/r)}{\partial z}\right]. \quad \text{(A2)}$$

Species mass fraction:

$$\rho U\frac{\partial m}{\partial x}+\rho W\frac{\partial m}{\partial z}=\frac{1}{r}\frac{\partial}{\partial z}\left[r\frac{\mu_{\text{eff}}}{\sigma_{\text{eff}}}\frac{\partial m}{\partial z}\right]. \quad \text{(A3)}$$

The turbulence model

Turbulent viscosity:

$$\frac{\mu_{\text{eff}}}{\sigma_{\text{eff}}}=\frac{\mu}{\sigma}+\frac{\mu_t}{\sigma_t} \quad \mu_t=C_\mu\rho k^2/\varepsilon. \quad \text{(A4)}$$

Turbulent mass diffusivity:

$$\Gamma_t=\mu_t/0.9\rho. \quad \text{(A5)}$$

Turbulence kinetic energy:

$$\rho U\frac{\partial k}{\partial x}+\rho W\frac{\partial k}{\partial z}=\frac{1}{r}\frac{\partial}{\partial z}\left[r\left(\frac{\mu_t}{\sigma_k}+\mu\right)\frac{\partial k}{\partial z}\right] +\mu_t\left[\left(\frac{\partial U}{\partial z}\right)^2+\left(r\frac{\partial V_\theta/r}{\partial z}\right)^2\right]-\rho\varepsilon-2\mu\left(\frac{\partial k^{1/2}}{\partial z}\right)^2. \quad \text{(A6)}$$

Turbulence energy dissipation:

$$\rho U\frac{\partial \varepsilon}{\partial x}+\rho W\frac{\partial \varepsilon}{\partial z}=\frac{1}{r}\frac{\partial}{\partial z}\left[r\left(\frac{\mu_t}{\sigma_\varepsilon}+\mu\right)\frac{\partial \varepsilon}{\partial z}\right] +C_1\frac{\varepsilon\mu_t}{k}\left[\left(\frac{\partial U}{\partial z}\right)^2+\left(r\frac{\partial V_\theta/r}{\partial z}\right)^2\right]-C_2\frac{\rho\varepsilon^2}{k} +C_3\nu\mu_t\left\{\frac{\partial}{\partial z}\left[\left(\frac{\partial U}{\partial z}\right)^2+\left(r\frac{\partial V_\theta/r}{\partial z}\right)^2\right]^{1/2}\right\}^2 \quad \text{(A7)}$$

where $C_\mu = 0.09\exp[-3.4/(1+R_t/50)^2]$
$C_2 = 1.92[1.0-0.3\exp(-R_t^2)]$

and $R_t=\rho k^2/\varepsilon$, the turbulent Reynolds number. The other empirical coefficients take the following values;

$$C_1=1.44;\quad C_3=2.0;\quad \sigma_k=1.0;\quad \sigma_\varepsilon=1.3.$$

Boundary conditions are applied at the disc surface ($z=0$) and beyond the edge of the boundary layer as follows:

$$z=0:\quad U=k=\varepsilon=0;\quad V_\theta=\omega r;\quad m=m_{\text{wall}}.$$
$$z=\infty:\quad U=k=\varepsilon=V_\theta=0;\quad m=m_\infty.$$

The above coefficients take the above values on the basis of extensive computer optimization as reported in [1, 7] and the author's extensive numerical experimentation with a wide variety of flow situations [8], including for example, flow over a flat plate; high and low Reynolds number flow in pipes and rectangular channels; flow between converging plates (sink flows).